Vibrotactile Haptic Feedback for Intuitive Control of Robotic Extra Fingers

Irfan Hussain[1], Leonardo Meli[1,2], Claudio Pacchierotti[1,2], Gionata Salvietti[2], and Domenico Prattichizzo[1,2]

Abstract— **Wearable robots have been mostly designed as exoskeletons, with segments and joints corresponding to those of the person they are coupled with. Exoskeletons are mainly employed to augment human body force and precision capabilities, or for rehabilitation purposes. More recently, new wearable robots resembling additional robotic limbs have been developed thanks to the progress in miniaturization and efficiency of mechanical and sensing components. However, wearable robotic extra limbs presented in the literature lack of effective haptic feedback systems. In this paper, we present a robotic extra finger coupled with a vibrotactile ring interface. The human user is able to control the motion of the robotic finger through a switch placed on the ring, while being provided with vibrotactile feedback about the forces exerted by the robotic finger on the environment. To understand how to control the vibrotactile interface to evoke the most effective cutaneous sensations, we executed perceptual experiments to evaluate its absolute and differential thresholds. We also carried out a pick-and-place experiment with ten subjects. Haptic feedback significantly improved the performance in task execution in terms of completion time, exerted force, and perceived effectiveness. All subjects preferred experimental conditions employing haptic feedback with respect to those not providing any force feedback.**
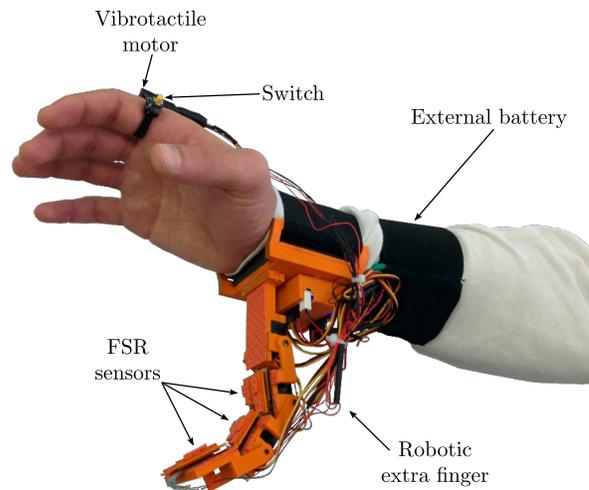
Fig. 1. The robotic extra finger together with the vibrotactile interface ring. The ring provides haptic feedback through a vibrating motor and enables the user to start and stop the finger motion through a switch.

I. INTRODUCTION

Wearable robots can potentially interact and collaborate with people in an intelligent environment [1]. In the last decades, wearable robots have been mostly designed as mechatronic systems shaped around and in function of the human body, with segments and joints corresponding to those of the person they were externally coupled with [2]. These systems have been often referred to as exoskeletons, whose main purposes are enhancing human body force and precision capabilities [3] or helping in rehabilitation processes [4].

The progress in miniaturization and efficiency of the mechanical and sensing components is extending the field of wearable robotics toward new devices which do not replicate or assist a part of the human body, but can rather be seen as robotic extra limbs. In [5], [6], two additional robotic arms, worn through a backpack-like harness, have been presented as possible device to assist human workers in aircraft assembly by holding an object, manipulating a workpiece, etc.. Although the principle is very promising, finding a trade off between wearability, efficiency and performance on such bulky robots still represents an open challenge.

Wearability is the key concept in the design of these type of devices. For this reason, we decided to augment the functions of the human hand, instead of developing additional robotic arms as in [5]. The goal is to integrate the human hand with an additional robotic finger as represented in Fig. 1. The availability of one or more extra fingers enhances the capabilities of the human hand in terms of workspace and in terms of manipulation capabilities. The extra finger increases the workspace volume, so that the augmented hand can, for instance, grasp objects that are anatomically impossible to grasp using one hand, or even manipulate more objects at the same time. In [7], we presented a 4 Degrees of Freedom (DoFs) modular device that can be worn on the wrist by means of an elastic band. Each module was actuated with servomotor and controlled by PWM with an Arduino board. Differently from [8], the design was highly focused on the wearability and portability of the system.

Beyond design guidelines, another interesting issue is how to interface the extra finger with the human hand motion. In [9], we presented a possible control strategy able to transfer to one or more extra fingers a part or the whole motion of the human hand. We considered an extension of the mapping method proposed in [10], [11] to the case of a human hand augmented with a robotic extra finger. A commercial dataglove was used to measure the hand configuration during a grasping task. Although this control approach guarantees a reliable tracking of the human hand and can be extended to more fingers, there are two main drawbacks to be solved. First, the user lacks a feedback of the robotic finger status and can only perceive the force
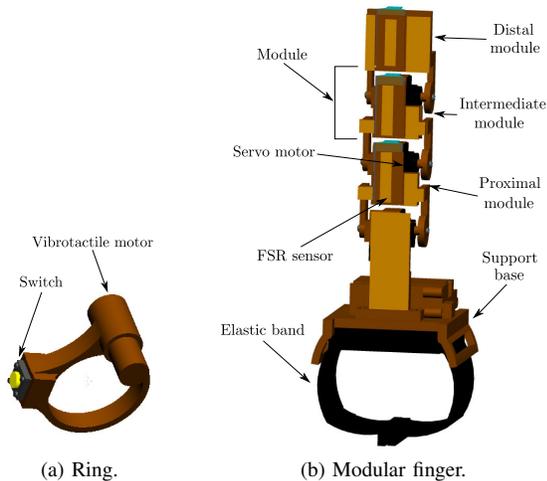
Fig. 2. CAD models of the vibrotactile interface and of the modular finger. Three single DoF modules are connected to a wrist elastic band. The ring is equipped with a push button which is used as an interface with the user and a vibrotactile motor to provide an haptic stimulus.

exerted by the device mediated by the grasped object. The second problem is related to the approaching phase of the grasp. In fact, the algorithm presented in [9] considers the motion of the whole hand to compute the motion of the extra finger, thus limiting the possibility of the user to make fine adjustments to adapt the finger shape to that of the grasped object.

In this work, we addressed these issues by introducing a vibrotactile interface that can be worn as a ring. The human user receives information through the vibrotactile interface about the robotic finger status in terms of contact/no contact with the grasped object and in terms of force exerted by the device. Haptic stimuli have been indeed proved to enhance the performance of robotic systems in many scenarios [12], [13], [14], [15]. However, most robotic systems with force reflection provide force feedback through grounded haptic devices, such as the Omega (Force Dimension, Switzerland) interfaces. Although these devices can be very accurate and able to provide a wide range of forces, their form factor makes them not suitable to be used in wearable applications, where the system needs to be lightweight, small, and easy to wear [16]. For this reason, we designed a custom wearable vibrotactile interface, since vibrotactile stimuli convey rich information and have an extremely compact form factor with respect to more popular grounded interfaces [17], [18], [19], [20].

Regarding the grasp approaching phase, we introduce a new control strategy that enables the finger to autonomously adapt to the shape of the grasped object. We developed a new finger prototype with 3 DoFs and three modules to resemble the kinematics of the human finger. Each module has been equipped with a force sensor able to detect contacts with the grasped object. We defined a grasping procedure that starts from a predefined position, when the robotic finger is open at its maximum. As soon as one module is in contact with the object, that module stops its motion, while the others keep moving toward the object. The details

of the closing procedure will be described in Sec. II. The procedure can be activated by pressing the switch placed on the interface ring (see Fig. 1). This approach dramatically simplifies the interaction with the robotic finger, reducing it to the activation of a grasping procedure through the wearable switch. This shared autonomy between the user and the device has been kept also in the control of the exerted force. We developed a variable compliance control that let the finger adapt its stiffness according to the force necessary to guarantee a stable grasp. The user is provided through the vibrating ring with information about the exerted forces and, therefore, about the finger compliance.

We tested the system in a pick and place task where users were asked to move an object between two predefined positions by taking advantage of the extra finger. We demonstrated that haptic feedback, together with the intuitive human robot interface, enhances users' performance in terms of completion time and exerted force.

The rest of the paper is organized as it follows. Section II describes the extra finger and the ring interface. Section III presents two preliminary experiments aiming at evaluating the absolute and differential thresholds of our vibrotactile haptic device. Section IV deals with the pick-and-place experiment carried out to evaluate the effectiveness of the system, while in Section V conclusion and future work are outlined.

II. THE EXTRA FINGER ROBOTIC DEVICE

A. System design

The robotic finger has a modular structure. Each module consists of a servomotor (HS-53 Microservo, HiTech, Korea) and a 3D printed plastic part with dimensions of $42 \times 33 \times 16$ mm. The prototype presented in this paper has 3 DoFs, that are obtained by considering three modules in a pitch-pitch connection. These modules replicate the flexion/extension motion of the human fingers.

A Force Sensing Resistor (FSR) (408, Interlink Electronics Inc., USA) was placed on each module, as reported in Fig. 2. These sensors will be used for the closing procedure and the compliance variation described in Sec. II-B. The finger is attached to a support base that can be worn on the wrist by means of an elastic band. We placed the device on the wrist center to enlarge the hand workspace [7].

The vibrotactile ring interface is designed to be worn on the index finger of the human hand, see Fig. 1. The ring is equipped with a switch and a vibro motor, as shown in Fig. 2. The ring housing is 3D printed. The motor used is an eccentric rotating mass vibrotactile motor (Precision MicroDrives, United Kingdom). The switch is used to start the finger closing procedure, as described in Sec. II-B, and move the finger back to the initial grasp position. The vibrotactile motor is used to provide vibrotactile feedback, as explained in Sec. IV.

The module actuator is controlled by PWM signal generated by an Arduino Nano board. The servos position feedback and FSRs signals are interfaced with the analog channels of the Arduino. An external battery is used to provide power to all the circuits (similarly to .
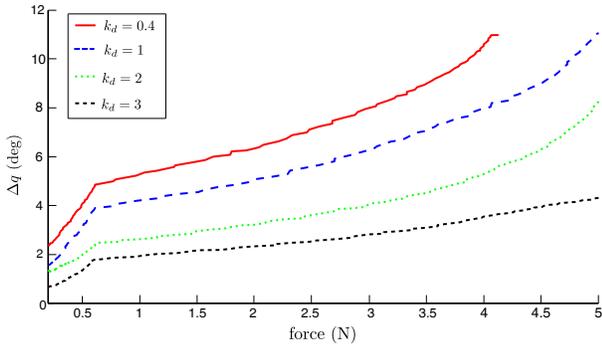
Fig. 3. Compliance behavior of a single module with different value of k_d. Force vs displacement is plotted. The force is measured using FSR sensor and the displacement is recorded by the position feedback of the modified servo motor.

Fig. 4. Performance characteristics of the Precision Microdrives 4 mm Vibration Motor (11 mm type).

B. Grasping procedure and compliance regulation

The user can command the finger motion by using the wearable switch placed on the ring. When the switch is activated, the finger starts to close with a fixed joint angle increment, equal in each module, from a predefined position. We considered the completely extended finger as the starting position to enlarge the set of possible graspable objects.

During the grasping phase, the FSR sensors are in charge of detecting the contact of each module with the grasped object. In order to have suitable contact points, we set different closing priorities for each module. If the distal module (see Fig. 2b) comes in contact first, the remaining two modules stop. If the intermediate module gets in contact first, only the proximal one stops, while the distal module keeps moving. Finally, if the proximal module comes in contact first, two different behaviors can occur: (1) the intermediate module gets in contact first and the distal one is free to move to get in contact with the object, (2) the distal module comes in contact first and then also the intermediate one stops. The grasping procedure is commanded by the user acting on the switch. When the grasp is complete, the finger starts to autonomously keep the grasp stable. This grasp stabilization is obtained by controlling the compliance of each module.

We modified the servomotor in order to read the joint position from the embedded potentiometer and we introduced a scaling factor k_d to modulate the displacement of the joint related to the applied force. The compliant behavior of a module with different values of the scaling factor k_d is reported in Fig. 3. The force at each module is measured by using the FSR sensor. The compliance decreases with the increase of k_d. The basic idea is that the module can change its compliance according to the force observed by each module through the relative FSR sensor. Thus, when the user pushes the object toward the extra finger to tight the grasp, the device becomes stiffer. The possibility to independently regulate each module's compliance allows to adapt the finger to the the shape of the grasped object also during manipulation tasks. Similar to what we did for the grasping procedure, we set the same priorities between the three modules also regarding the compliance variation.

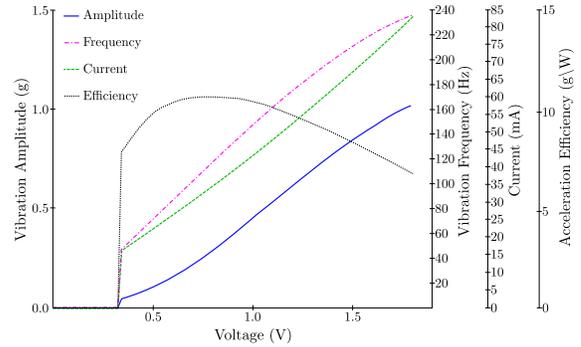When the user wants to release the grasped object, he just

needs to lower the force exerted by his hand on the object and, automatically, the robotic device will make its joints more compliant. Eventually, by pressing again the switch, the robotic finger moves back to its home position by following a predefined trajectory.

III. PERCEPTUAL THRESHOLDS

In order to understand how to drive the vibrotactile ring correctly to evoke the most effective cutaneous sensations, we ran two preliminary experiments aiming at evaluating the absolute and differential thresholds of our device. The motor we use is an eccentric rotating mass vibrotactile motor, and it is not possible to separately control amplitude and frequency of vibration. The relationship between input voltage, and the amplitude and frequency of the vibration is shown in Fig. 4.

Subjects were required to wear the vibrotactile ring on their right index proximal phalanx. Moreover, to avoid any additional cue, subjects were blindfolded and wore noise-canceling headphones.

Absolute threshold

The absolute threshold can be defined as the "smallest amount of stimulus energy necessary to produce a sensation" [21], and it gives us information about the smallest vibration we need to provide in order to produce a perceivable sensation by the human user.

Six participants took part in the experiment. The experimenter explained the procedures and spent about three minutes adjusting the setup to be comfortable before the subject began the experiment.

We evaluated the absolute threshold by using the simple up-down method [22]. We used a step-size of 0.08 V, which reduced of 0.02 V every reversal. We considered the task completed when four reversals occurred. Subjects were required to wear the cutaneous device as shown in Fig. 1 and tell the experimenter when they felt the stimulus.

Each participant performed forty-eight repetitions of the simple up-down procedure, with six repetitions for each considered duration of the vibratory stimulus: 13 ms, 25 ms, 37 ms, 50 ms, 100 ms, 150 ms, 200 ms, and 250 ms. Fig. 5 shows the absolute thresholds averaged over all subjects.
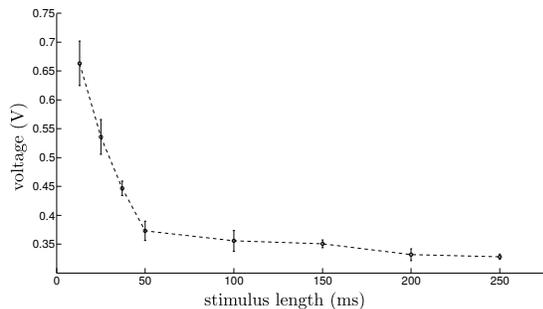
Fig. 5. Absolute threshold. Mean values and standard errors of the mean (SEM) are plotted. The relationship between input voltage, and the amplitude and frequency of the vibration can be found in Fig. 4.
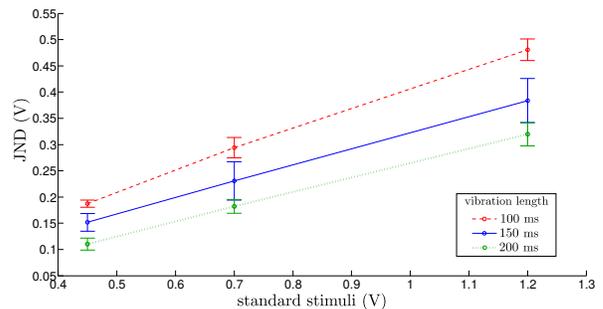

Fig. 6. Differential threshold. Mean values and standard errors of the mean (SEM) are plotted. The relationship between input voltage, and the amplitude and frequency of the vibration can be found in Fig. 4.

Differential threshold

The differential threshold can be in turn defined as "the smallest amount of stimulus change necessary to achieve some criterion level of performance in a discrimination task" [21]. This gives us information about how much different two vibrations provided with our device need to be in order to be perceived as different by the human user. This threshold is often referred to as just-noticeable difference or JND. The differential threshold of a perceptual stimulus reflects also the fact that people are usually more sensitive to changes in weak stimuli than they are to similar changes in stronger or more intense stimuli. The German physician Ernst Heinrich Weber suggested the simple proportional law $JND = kI$, suggesting that the differential threshold increases by increasing the intensity I of the stimulus. Constant k thus referred to as "Weber's fraction".

The experimental setup was the same as described in Sec. III. Nine participants took part in this experiment. As in Sec. III, the experimenter explained the procedures and spent about three minutes adjusting the setup to be comfortable before the subject began the experiment. We evaluated the differential threshold using again the simple up-down method [22]. We used again a step-size of 0.08 V, which reduced of 0.02 V at every reversal. We considered the task completed when four reversals occurred. Subjects were required to wear the cutaneous device and tell the experimenter when the two vibrations provided felt different. We tested the JND at three reference stimuli: 0.45 V, 0.7 V, and 1.2 V, which corresponded, respectively, to vibrations of amplitude 0.15 g, 0.30 g, and 0.62 g, and of frequency 68 Hz, 100 Hz, and 160 Hz (see Fig. 4). We considered also three different vibration lengths: 100 ms, 150 ms, and 200 ms. We did not consider lengths < 100 ms to be sure that everyone would be able to perceive them at all reference stimuli (see Fig. 5). The results observed are in agreement with previous results in the literature [23].

Each participant performed eighteen trials of the up-down procedure, with two repetitions for each of reference stimulus and vibration length considered. Fig. 6 shows the differential thresholds averaged over all subjects. For the reference stimuli of 0.45 V, 0.7 V, and 1.2 V, and a vibration length of 100 ms, the average JNDs are 0.19 V, 0.29 V, and 0.48 V, respectively. Thus, the Weber fractions are 0.42, 0.42 and 0.40, respectively, following Weber's Law. For the reference stimuli of 0.45 V, 0.7 V, and 1.2 V, and a vibration length of 150 ms, the average JNDs are 0.15 V, 0.23 V, and 0.38 V, respectively. Thus, the Weber fractions are 0.34, 0.33 and 0.32, respectively, following Weber's Law. Finally, for the reference stimuli of 0.45 V, 0.7 V, and 1.2 V, and a vibration length of 200 ms, the average JNDs are 0.11 V, 0.18 V, and 0.32 V, respectively. Thus, the Weber fractions are 0.25, 0.26 and 0.27, respectively, following Weber's Law.

IV. EXPERIMENTAL EVALUATION

In order to evaluate the effectiveness of our extra finger device and the usefulness of vibrotactile haptic feedback, we carried out a pick-and-place experiment. The experimental setup was composed of our robotic extra finger device, the vibrotactile ring, and a cylinder, as shown in Fig. 7. The cylinder was made of ABSPlus, it had a radius of 7.5 cm, a height of 15 cm, and a weight of 150 g. The robotic extra finger device was controlled as detailed in Sec. II-B. The task consisted of grasping the cylinder, lifting it from the table, and moving it 45 cm right, being as fast as possible. The initial and final positions of the cylinder were marked on the table by two red circles (see Fig. 7). An extended version of the video of the experiment can be downloaded at http://goo.gl/h34FjF.

Ten participants took part in the experiment. The experimenter explained the procedures and spent about five minutes adjusting the setup to be comfortable before the subject began the experiment. Each participant made twenty randomized trials of the pick-and-place task, with five repetitions for each feedback condition proposed:

- vibration bursts on making and breaking contact with the grasped object and when close to the actuators' force limit (condition V_{mb}),
- vibration bursts on the intensity of the force exerted by the robotic finger (condition V_t),
- continuous vibrations proportional to the intensity of the force exerted by the robotic finger (condition V_c),
- no haptic feedback at all (condition N).

In condition V_{mb}, the vibrotactile ring provided a 200 ms-long vibration on making and breaking contact with the cylinder. Moreover, it also provided a 200 ms-long vibration when the force exerted by the robotic finger was close to the maximum force that actuators could provide at the fingertip (i.e., 5 N). The amplitude and frequency of these vibrations
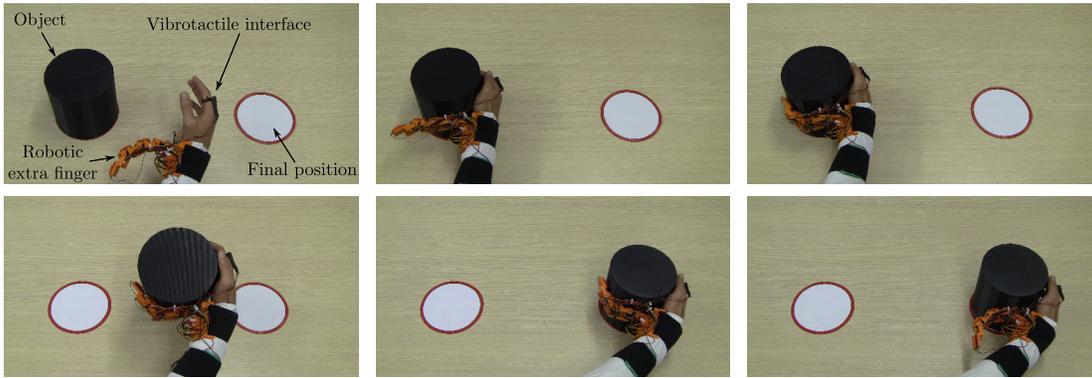
Fig. 7. Experimental setup. The task consisted of grasping the cylinder from its starting position, lifting it from the table, and moving it to its final position, being as fast as possible. The cylinder had a radius of 7.5 cm and a height of 15 cm.

were set to 0.30 g and 100 Hz, respectively, so to be easy to recognize (input voltage $v_i = 0.7$ V, see Sec. III).

In condition V_t, the vibrotactile ring provided 200 ms-long vibrations on making and breaking contact with the cylinder and when the force sensed by the robotic finger was equal to 2 N and 4 N (we considered the maximum force sensed among the three sensors). On the making and breaking contact, the amplitude and frequency of the vibrations were set to 0.30 g and 100 Hz, respectively, as in condition V_{mb} (input voltage $v_i = 0.7$ V). On the other hand, when the force sensed by the robotic finger was 2 N and 3 N, the vibrotactile motor was provided with inputs v_i of 0.9 V (amp. 0.43 g, freq. 124 Hz) and 1.7 V (amp. 0.94 g, freq. 222 Hz), respectively. Amplitude values and force thresholds were chosen to be easy to distinguish (see Sec. III) and fit the vibrotactile motor specifications (see Fig. 4).

In condition V_c, the vibrotactile ring provided continuous vibrotactile feedback proportional to the intensity of the force exerted by the robotic finger. The commanded input voltage v_i, proportional to the mean force sensed on the robotic finger, was evaluated as

$$v_i = \frac{(f_{e,max} + 0.3)}{2.5},$$

where $f_{e,max}$ is the maximum force registered among the three sensors on the robotic finger. The relationship between input voltage v_i and the amplitude and frequency of the vibration can be found in Fig. 4. For example, when the sensors register an average force of 2 N, the vibrotactile ring provides a vibration of amplitude 0.43 g and frequency 124 Hz (as in condition V_t). No vibration was provided when the robotic finger was not in contact with the object.

In condition N, no haptic feedback was provided.

Completion time and mean exerted forces provided a measure of performance. A low value of these metrics denotes the best performance. The time started to be recorded when the semi-autonomous grasping phase was completed and the user lifted the object, and it stops when the object was placed on its final position.

Fig. 8a shows the average task completion time. All the data passed the Shapiro-Wilk normality test and the Mauchly's Test of Sphericity. A repeated-measure ANOVA showed a statistically significant difference between the

means of the four feedback conditions (F(3,27) = 16.597, $p < 0.001$, a = 0.05). Post hoc analysis with Bonferroni adjustments revealed a statistically significant difference between condition N and all the others (N vs. V_{mb}, $p = 0.002$; N vs. V_t, $p = 0.027$; N vs. V_c, $p = 0.014$).

Fig. 8b shows the average exerted force, evaluated as the mean over time of $f_{e,max}$. All the data passed the Shapiro-Wilk normality test. Mauchly's Test of Sphericity indicated that the assumption of sphericity had been violated ($\chi^2(2) = 17.008, p < 0.001$). A repeated-measure ANOVA with Greenhouse-Geisser correction showed a statistically significant difference between the means of the four feedback conditions (F(1.482,13.340) = 12.015, $p = 0.002$, a = 0.05). Post hoc analysis with Bonferroni adjustments revealed again a statistically significant difference between condition N and all the others (N vs. V_{mb}, $p = 0.032$; N vs. V_t, $p = 0.025$; N vs. V_c, $p = 0.015$).

In addition to the quantitative evaluation reported above, we also measured users' experience. Immediately after the experiment, subjects were asked to report the effectiveness of each feedback condition in completing the given task using bipolar Likert-type seven-point scales. Fig. 8c shows the perceived effectiveness of the four feedback conditions. A Friedman test showed a statistically significant difference between the means of the four feedback conditions ($\chi^2(3) = 27.903$, $p < 0.001$). The Friedman test is the non-parametric equivalent of the more popular repeated measures ANOVA. The latter is not appropriate here since the dependent variable was measured at the ordinal level. Post hoc analysis with Bonferroni adjustments revealed a statistically significant difference between conditions N and V_{mb} ($p < 0.001$), N and V_c ($p = 0.001$), and V_t and V_{mb} ($p = 0.008$). Moreover, although condition V_t was not found significantly different from condition V_c, comparison between them was very close to significance ($p = 0.072$). Finally, subjects were asked to choose the condition they preferred the most. Condition V_{mb} was preferred by six subjects and condition V_c was preferred by four subjects.

V. CONCLUSION AND FUTURE WORK

In this paper, we presented the integration of the wearable robotic extra finger with a ring able to provide vibrotactile
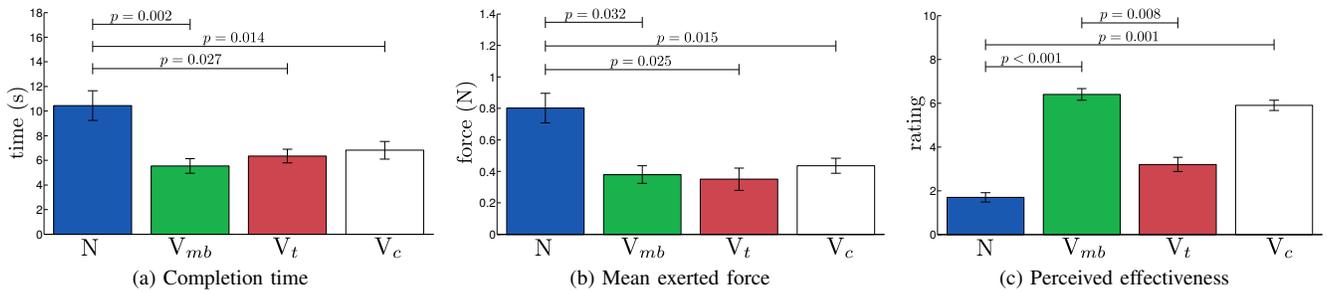
Fig. 8. Pick-and-place experiment. Completion time, mean exerted force, and perceived effectiveness for conditions providing vibration bursts on making and breaking contact and when close to the actuators' force limit (V_{mb}), vibration bursts on the intensity of the force exerted (V_t), continuous vibrations proportional to the intensity of the force exerted (V_c), and no haptic feedback (N). Mean and Standard Error of the Mean (SEM) are plotted.

haptic feedback. We introduced also a new solution for the grasping phase based on a wearable switch embedded in the ring and a closing policy that let the robotic finger adapt to the object's shape. In order to evaluate the effectiveness of our extra finger device and the usefulness of vibrotactile haptic feedback, we carried out a pick-and-place experiment. Ten subjects were asked to grasp a cylinder, lift it, and move it 45 cm right, being as fast as possible. Haptic feedback significantly improved the performance of the task in terms of completion time, exerted force, and perceived effectiveness. Moreover, all subjects preferred conditions employing haptic feedback. Within the conditions employing haptic feedback, no statistical difference was found in terms of completion time and force exerted. However, conditions V_{mb} and V_c were perceived as more effective than V_t. This may be due either to a saturation effect on the skin receptors or to the fact that the very rich information provided in condition V_t can be difficult to be understood by the user.

In the future, we are planning to replace the FSR sensors with more accurate sensors able to measure both forces and torques. Moreover, we are going to investigate how providing vibrotactile stimuli to other parts of the body (e.g., the wrist, the forearm) affect the performance of the given task. Finally, we will extensively test our device in more challenging real-life scenarios, such as grasp compensation for post-stroke patients.

REFERENCES

[1] S. Mohammed and Y. Amirat, "Towards intelligent lower limb wearable robots: Challenges and perspectives - state of the art," in *Proc. IEEE Int. Conf. on Robotics and Biomimetics*, pp. 312–317, 2009.

[2] J. L. Pons *et al.*, *Wearable robots: biomechatronic exoskeletons*, vol. 338. Wiley Online Library, 2008.

[3] A. B. Zoss, H. Kazerooni, and A. Chu, "Biomechanical design of the berkeley lower extremity exoskeleton (bleex)," *IEEE/ASME Transactions on Mechatronics*, vol. 11, no. 2, pp. 128–138, 2006.

[4] A. Gupta and M. K. O'Malley, "Design of a haptic arm exoskeleton for training and rehabilitation," *IEEE/ASME Transactions on Mechatronics*, vol. 11, no. 3, pp. 280–289, 2006.

[5] F. Parietti, K. Chan, and H. H. Asada, "Bracing the human body with supernumerary robotic limbs for physical assistance and load reduction," in *Proc. IEEE Int. Conf. on Robotics and Automation*, pp. 141–148, 2014.

[6] F. Parietti and H. H. Asada, "Dynamic analysis and state estimation for wearable robotic limbs subject to human-induced disturbances," in *Proc. IEEE Int. Conf. on Robotics and Automation*, pp. 3880–3887, 2013.

[7] D. Prattichizzo, M. Malvezzi, I. Hussain, and G. Salvietti, "The sixth-finger: a modular extra-finger to enhance human hand capabilities," in *Proc. IEEE Int. Symp. in Robot and Human Interactive Communication*, 2014.

[8] F. Wu and H. Asada, "Bio-artificial synergies for grasp posture control of supernumerary robotic fingers," in *Proc. of Robotics: Science and Systems*, 2014.

[9] D. Prattichizzo, G. Salvietti, F. Chinello, and M. Malvezzi, "An object-based mapping algorithm to control wearable robotic extra-fingers," in *Proc. IEEE/ASME Int. Conf. on Advanced Intelligent Mechatronics*, 2014.

[10] G. Gioioso, G. Salvietti, M. Malvezzi, and D. Prattichizzo, "Mapping synergies from human to robotic hands with dissimilar kinematics: an approach in the object domain," *IEEE Trans. on Robotics*, 2013.

[11] G. Salvietti, M. Malvezzi, G. Gioioso, and D. Prattichizzo, "On the use of homogeneous transformations to map human hand movements onto robotic hands," in *Proc. IEEE Int. Conf. on Robotics and Automation*, pp. 5352–5357, 2014.

[12] M. J. Massimino and T. B. Sheridan, "Teleoperator performance with varying force and visual feedback," *Human Factors: The Journal of the Human Factors and Ergonomics Society*, vol. 36, no. 1, pp. 145–157, 1994.

[13] D. Prattichizzo, C. Pacchierotti, and G. Rosati, "Cutaneous force feedback as a sensory subtraction technique in haptics," *IEEE Transactions on Haptics*, 2012.

[14] C. Pacchierotti, F. Chinello, M. Malvezzi, L. Meli, and D. Prattichizzo, "Two finger grasping simulation with cutaneous and kinesthetic force feedback," *Haptics: Perception, Devices, Mobility, and Communication. EuroHaptics.*, pp. 373–382, 2012.

[15] L. Moody, C. Baber, and T. N. Arvanitis, "Objective surgical performance evaluation based on haptic feedback," *Studies in Health Technology and Informatics*, pp. 304–310, 2002.

[16] D. Prattichizzo, F. Chinello, C. Pacchierotti, and M. Malvezzi, "Towards wearability in fingertip haptics: a 3-dof wearable device for cutaneous force feedback," *IEEE Transactions on Haptics*, vol. 6, no. 4, pp. 506–516, 2013.

[17] L. Meli, C. Pacchierotti, and D. Prattichizzo, "Sensory subtraction in robot-assisted surgery: fingertip skin deformation feedback to ensure safety and improve transparency in bimanual haptic interaction," *IEEE Transactions on Biomedical Engineering*, vol. 61, no. 4, pp. 1318–1327, 2014.

[18] R. E. Schoonmaker and C. G. L. Cao, "Vibrotactile force feedback system for minimally invasive surgical procedures," in *Proc. IEEE Int. Conf. on Systems, Man, and Cybernetics*, vol. 3, pp. 2464–2469, 2006.

[19] C. Cipriani, M. D'Alonzo, and M. C. Carrozza, "A miniature vibrotactile sensory substitution device for multifingered hand prosthetics," *IEEE Transactions on Biomedical Engineering*, vol. 59, no. 2, pp. 400–408, 2012.

[20] C. Pacchierotti, M. Abayazid, S. Misra, and D. Prattichizzo, "Teleoperation of steerable flexible needles by combining kinesthetic and vibratory feedback," *IEEE Transactions on Haptics*, vol. 7, no. 4, pp. 551–556, 2014.

[21] G. A. Gescheider, *Psychophysics: the fundamentals*. Psychology Press, 2013.

[22] H. Levitt, "Transformed up-down methods in psychoacoustics," *The Journal of the Acoustical society of America*, vol. 49, no. 2B, pp. 467–477, 1971.

[23] E. Arabzadeh, C. W. Clifford, and J. A. Harris, "Vision merges with touch in a purely tactile discrimination," *Psychological Science*, vol. 19, no. 7, pp. 635–641, 2008.